



# Polydimethylsiloxane-based permeation passive air sampler. Part I: Calibration constants and their relation to retention indices of the analytes

Suresh Seethapathy, Tadeusz Górecki\*

Department of Chemistry, University of Waterloo, 200 University Avenue West, Waterloo, Ontario, Canada N2L 3G1

## ARTICLE INFO

### Article history:

Received 1 August 2010  
Received in revised form 28 October 2010  
Accepted 1 November 2010  
Available online 9 November 2010

### Keywords:

Sample preparation  
Permeation passive sampling  
Volatile organic compounds  
Calibration  
Uptake rate  
Linear temperature programmed retention index

## ABSTRACT

A simple and cost effective permeation passive sampler equipped with a polydimethylsiloxane (PDMS) membrane was designed for the determination of time-weighted average (TWA) concentrations of volatile organic compounds (VOCs) in air. Permeation passive samplers have significant advantages over diffusive passive samplers, including insensitivity to moisture and high face velocities of air across the surface of the sampler. Calibration constants of the sampler towards 41 analytes belonging to alkane, aromatic hydrocarbon, chlorinated hydrocarbon, ester and alcohol groups were determined. The calibration constants allowed for the determination of the permeability of PDMS towards the selected analytes. They ranged from  $0.026 \text{ cm}^2 \text{ min}^{-1}$  for 1,1-dichloroethylene to  $0.605 \text{ cm}^2 \text{ min}^{-1}$  for *n*-octanol. Further, the mechanism of analyte transport across PDMS membranes allowed for the calibration constants of the sampler to be estimated from the linear temperature programmed retention indices (LTPRI) of the analytes, determined using GC columns coated with pure PDMS stationary phases. Statistical analysis using Student's *t* test indicated that there was no significant difference at the 95% probability level between the experimentally obtained calibration constants and those estimated using LTPRI for most analyte groups studied. This correlation allows the estimation of the calibration constants of compounds not known to be present at the time of sampler deployment, which makes it possible to determine parameters like total petroleum hydrocarbons in the vapor phase.

© 2010 Elsevier B.V. All rights reserved.

## 1. Introduction

Passive sampling is an analytical chemistry tool used to achieve most of the basic sample preparation goals. These include, among others, isolation of the analytes from the matrix and their pre-concentration to increase the selectivity and sensitivity of the measurements, chemically changing the analyte to a form suitable for the analytical measurement, and/or reduction of, or complete elimination of solvent use (green chemistry). Górecki and Namieśnik defined passive sampling as “any sampling technique based on free flow of analyte molecules from the sampled medium to a collecting medium, as a result of a difference in chemical potential of the analyte between the two media” [1]. When the difference in chemical potential is solely due to the difference in the analyte concentrations between the two media, the analyte transfer can be conveniently explained based on Fick's laws of diffusion under a concentration gradient and the sampling does not require any external power like active sampling methods do.

Analyte transfer from the sampled medium to the collecting medium in a diffusive passive sampler takes place through a well-defined air volume (e.g. pores in a diffusive barrier), while in permeation-type samplers analytes pass through a polymer membrane driven by the concentration gradient between the two media. The sorbent is typically chosen to have high sorption capacity for the VOCs being sampled (a zero sink), which helps maintain the concentration gradient between the sampled medium and the collecting medium throughout the deployment duration. Factors such as high analyte/background matrix concentration and/or high humidity might lead to premature sorbent saturation, and consequently non-ideal functioning of the sampler. Since the diffusion coefficient of water molecules in air is considerably higher when compared to many VOCs, their uptake rate into diffusive-type samplers is also higher. This makes it difficult for such diffusive-type samplers to be used for soil gas measurements (with wide applicability in vapor intrusion and soil remediation studies), where humidity could often be close to 100%. Consequently, such samplers can be deployed in the field only for relatively short durations under high humidity conditions. The use of permeation-type passive samplers employing hydrophobic PDMS membranes can offset this problem (at least partially), as the permeability of water molecules through PDMS (and hence their uptake rate) is one to several orders

\* Corresponding author. Tel.: +1 519 888 4567x35374; fax: +1 519 746 0435.  
E-mail address: [tgorecki@uwaterloo.ca](mailto:tgorecki@uwaterloo.ca) (T. Górecki).

of magnitude lower than those for most VOCs. An added advantage of using such membranes is that high face velocities of air do not alter the uptake rates of the sampler. This is not the case with certain types of diffusive-type passive samplers, where strong air currents might effectively reduce the diffusive path length, and consequently increase the uptake rates. On the other hand, low air flow velocities across the sampler affect both types of samplers in a similar manner (so-called “starvation effect”) [2].

Zabiegała and co-workers took advantage of the favorable properties of PDMS membranes when designing badge type passive samplers used for various purposes [3–6]. The main disadvantage of these samplers was the requirement that the calibration constant be known prior to sampler deployment. This necessitated the analytes' identity to be known prior to the sampler deployment, which was not always possible. In such cases, it becomes important to be able to estimate the calibration constant for an analyte after analyzing the sorbent in the laboratory. For diffusive-type samplers, such estimation boils down to using either available or estimated diffusion coefficients of the analytes in air to calculate the calibration constants. Zabiegała and co-workers reported various estimation methods based on physicochemical properties of the analytes for permeation-type passive samplers using PDMS membranes [3]. One such estimation was based on the linear temperature-programmed retention index (LTPRI) of the analyte in a GC column coated with pure PDMS. The estimation of the calibration constant was possible in this case due to the similarities between the analyte transfer mechanism into the sampler and the separation mechanism in a capillary GC column using PDMS as the stationary phase.

Based on the work of Zabiegała and co-workers, a simplified and cost-effective permeation-type passive sampler was designed for this study based on a 2 mL crimp-cap gas chromatography autosampler vial equipped with a polydimethylsiloxane (PDMS) membrane and filled with a carbon-based adsorbent. Apart from the low material costs of the sampler and ease of fabrication, the design allows for potential automation of the extraction and chromatographic analysis for high-throughput analysis. The relationship between the calibration constant of the sampler and LTPRI was further studied theoretically and experimentally and is presented in this paper. The advantages of this design with respect to variations in humidity and temperature will be presented in the second part of this paper.

## 2. Theory

The idealized, steady state concentration profile of the permeating vapor in and around permeation-type samplers during deployment is shown in Fig. 1. According to Graham's solution–diffusion model for permeation of organic compounds, the transfer of gas or vapor across a polymer takes place in three steps: dissolution of the vapor molecule in the polymer, diffusion of the molecule under a concentration gradient through the polymer, and the release of the vapor from the polymer at the opposite side of the membrane [7,8]. Applying Fick's law to permeation-type passive samplers, the amount of analyte  $M$  (kg) collected in time  $t$  (min) by the sampler is given by

$$\left(\frac{M}{t}\right) = D \frac{A}{L_m} (C_{ma} - C_{ms}) \quad (1)$$

where  $D$  is the diffusion coefficient of the analyte in the membrane ( $\text{cm}^2 \text{min}^{-1}$ ),  $A$  is the surface area of the membrane ( $\text{cm}^2$ ),  $L_m$  is the membrane thickness (cm),  $C_{ma}$  is the concentration of the analyte on the surface of the membrane exposed to air ( $\text{kg}/\text{cm}^3$ ), and  $C_{ms}$  is the concentration of the analyte on the membrane surface in contact with the sorbent ( $\text{kg}/\text{cm}^3$ ).

The concentration of the analyte at the membrane–sorbent interface is practically zero due to removal of the analyte from the gas phase by the sorbent, hence  $C_{ms}$  is approximately zero. At a given temperature, the concentration of the analyte on the membrane surface that is exposed to the air and the concentration of the analyte in air are related to one another as follows:

$$C_{ma} = KC_0 \quad (2)$$

where  $K$  (dimensionless) is the partition coefficient of the analyte between the air and the membrane. Under the conditions of constant temperature, the diffusion coefficient, partition coefficient, as well as membrane area and thickness are all constant and can be replaced by a new constant,  $k$ .

$$k = \frac{L_m}{DKA} \quad (3)$$

where  $k$  is the calibration constant of the passive sampler. The product of the analyte's diffusion coefficient  $D$  in the membrane and its partition coefficient  $K$  is defined as the permeability of the polymer ( $P$ ,  $\text{cm}^2 \text{min}^{-1}$ ) towards that particular analyte, and defines the relative calibration constants of the passive sampler towards various analytes [9]. From Eqs. (1)–(3), one can calculate the concentration of the analyte ( $C_0$ ) in the sample when the amount collected by the sampler is experimentally determined and the exposure duration ( $t$ ) is known.

$$C_0 = \frac{kM}{t} \quad (4)$$

Zabiegała et al. determined the calibration constants of various groups of analytes and concluded that they were linearly related to LTPRI [3]. However, experiments performed in this research indicated that the relationship between the calibration constants and LTPRI did not match that published by Zabiegała et al. in a broader range of calibration constant values. In order to explain the discrepancy, the theoretical relationship between LTPRI and the calibration constants was examined and the hypothesis formulated was tested in this project.

It has long been known that vapor molecules permeate faster through rubbery polymers (such as PDMS) than through glassy polymers (such as Teflon<sup>®</sup>) [8]. PDMS, of all the rubbery polymers, has one of the lowest diffusivity selectivities for permeation because of the flexible (–Si–O–Si–) backbone of the polymer chains, as well as the relatively weak binding forces between the individual segments [10]. In fact, PDMS has one of the lowest glass-transition temperatures (146 K), with long-range segmental motions even at very low temperatures [8]. As a result, the relative differences in permeability of vapor molecules are mostly governed by their solubility (or, in other words, the partition coefficient) in the polymer rather than the diffusivity in the polymer [8]. Results of various studies reported in the literature support the assumption that diffusivity of molecules in PDMS is of the same order of magnitude for the majority of volatile organic compounds. This can be confirmed using data on diffusion and partition coefficients reported by Kong and Hawkes at 321 K [11]. Within the homologous series, the diffusion coefficients of the compounds decrease with increasing molecular size, but the relative decrease is marginal when compared to the exponential increase in the partition coefficients of the compounds. A mathematical relationship between the calibration constant and the partition coefficient can then be derived under the approximate assumption that  $D$  is constant for all volatile organic compounds. Under these conditions, taking the natural logarithms of both sides of Eq. (3), one gets,

$$\ln k = Z - \ln K \quad (5)$$

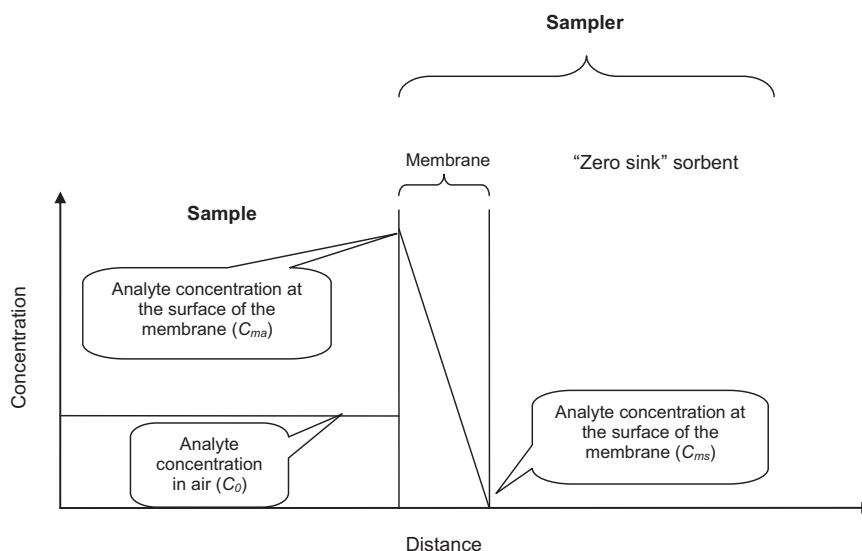


Fig. 1. Ideal, steady state concentration profile for permeation passive samplers during deployment.

where  $Z$  is a constant defined by:

$$Z = \ln \left[ \frac{L_m}{AD} \right] \quad (6)$$

In a homologous series of compounds, even though the diffusion coefficients are of the same order of magnitude, they typically decrease with increasing molecular weight of the compound. Under such conditions, constancy of the  $D \times MW$  product can also be considered, and the correlations explored. The assumption that the product of the diffusion coefficient and the molecular weight can be considered a constant was studied for the diffusion coefficients available from literature sources [11,12]. With this assumption, the mathematical relationship takes the form

$$\ln \left[ \frac{k}{MW} \right] = Q - \ln K \quad (7)$$

where  $Q$  is a constant defined as

$$Q = \ln \left[ \frac{L_m}{AD \times MW} \right] \quad (8)$$

Eqs. (5) and (7) show the relationships between the calibration constant and the partition coefficient. Calibration constant can then be related to LTPRI based on the relationship between LTPRI and the partition coefficient. Partition gas chromatography involves the partitioning of the solute between a liquid stationary phase and a gaseous mobile phase. Therefore, the retention properties of a compound in such a chromatographic separation are a function of the analyte partition coefficient between the carrier gas and the stationary phase (PDMS in this case). Under isothermal conditions, the partition coefficient of a solute at a given temperature is related to the retention time of the solute in the following manner [13]:

$$\frac{t'_r}{t_m} = \frac{t_r - t_m}{t_m} = K \frac{V_s}{V_m} \quad (9)$$

where  $t'_r$  is the adjusted retention time,  $t_m$  is the retention time of a non-retained compound,  $t_r$  is the retention time of the solute,  $K$  is the partition coefficient of the solute,  $V_s$  is the volume of the stationary phase, and  $V_m$  is the volume of the mobile phase. Van Den Dool and Kratz [14] introduced the concept of LTPRI (dimensionless), which involves calculation of the retention index while achieving chromatographic separation under the conditions of linear temperature programming. LTPRI is defined as:

$$\text{LTPRI} = 100 \left[ \frac{t_r - t_n}{t_{n+1} - t_n} \right] + 100n \quad (10)$$

where  $t_r$  is the retention time of the analyte,  $t_n$  is the retention time of the  $n$ -alkane eluting directly before the analyte,  $t_{n+1}$  is the retention time of the  $n$ -alkane eluting directly after the analyte, and  $n$  is the number of carbon atoms in the  $n$ -alkane eluting directly before the analyte. The exact correlation between LTPRI and the partition coefficient is complicated, and involves fluid dynamics inside the capillary column [15]. However, various researchers working on determining empirical relationships and/or mathematical approximations have found that LTPRI for a homologous series of compounds is related to the partition coefficient of the analytes at a particular temperature as follows [16]:

$$\text{LTPRI} = N \ln K + B \quad (11)$$

where  $N$  and  $B$  are constants. The relationship for a homologous series of  $n$ -alkanes can be verified using data obtained by Kłoskowski et al. at 298 K using a capillary column with PDMS stationary phase [17]. Further validity of this concept can be drawn from data presented by Martos et al., who used solid phase microextraction techniques for compounds including benzene, toluene, ethyl benzene,  $n$ -propyl benzene,  $n$ -pentyl benzene and  $n$ -hexyl benzene among others. The above relationship was successfully used to estimate the calibration constants of various analytes in solid-phase microextraction with PDMS-coated fibers. From Eqs. (5), (7) and (11), the relationship between the calibration constant  $k$  and LTPRI can theoretically be obtained and can be studied under two scenarios:

**Case 1:** When  $D$  is assumed to be constant, Eqs. (5) and (11) suggest that  $\ln(k)$  is directly proportional to LTPRI. If this is true, then the major advantage would be the ability to estimate the calibration constants for analytes without knowing their identity (because it is not required to know the identity of a compound to determine its LTPRI).

**Case 2:** When  $\ln(D \times MW)$  is considered constant, Eqs. (7) and (11) suggest that  $\ln(k/MW)$  is directly proportional to LTPRI. In this case, the calibration constant could be estimated using LTPRI, but the identity of the compound would have to be known in order to determine its molecular weight. The identities of unknown analytes (thus their molecular weights) can often be established when using mass spectrometry for analyte detection.

It should be noted that the physical form of PDMS within the capillary column may differ from that which forms the membrane. Nevertheless, Cramers et al. noted that the LTPRI was nearly the same on PDMS stationary phases with and without

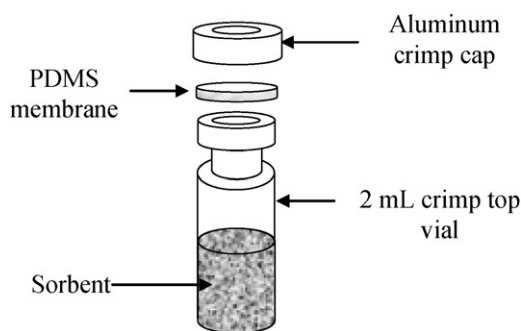


Fig. 2. Crimp cap vial-based permeation passive sampler (WMS sampler).

cross-linking [18]. Furthermore, Zabiegała et al. showed that LTPRI determined using different gas chromatographs and different capillary columns (with PDMS stationary phase) were nearly the same [19]. Therefore, the hypothesis that the calibration constant should be related to LTPRI should still be valid.

### 3. Experimental

#### 3.1. Chemicals

High purity CS<sub>2</sub> required for the preparation of standard solutions of the analytes for gas chromatographic quantification and for analyte desorption from sorption tubes and passive samplers was purchased from VWR CANLAB (Mississauga, ON). Chromatography grade compressed air, helium, nitrogen and hydrogen were purchased from Praxair (Kitchener, ON). All high purity, analytical grade chemicals were purchased from Sigma–Aldrich (Bellefonte, PA). The analytes were *n*-alkanes (*n*-hexane to *n*-decane), aromatic hydrocarbons (benzene, toluene, ethylbenzene, *o*-xylene, propylbenzene and butylbenzene), chlorinated compounds (chloromethanes, 1,1-dichloroethylene, *cis*-1,2-dichloroethene, 1,2-dichloroethane, 1,1,1-trichloroethane, and trichloroethene), alcohols (*n*-butanol to *n*-octanol, 2-methyl-1-propanol, 2,3-dimethyl-3-pentanol, 2,4-dimethyl-3-pentanol, 2-ethyl-1-hexanol, 2-methyl-1-butanol, 6-methyl-2-heptanol, 2-hexanol, 2-octanol and 3 octanol), and esters (ethyl acetate, propyl acetate, butyl acetate, *sec*-butyl acetate, methyl butyrate, ethyl butyrate, propyl butyrate and butyl butyrate).

#### 3.2. Passive sampler design

The passive sampler was designed and fabricated using a 2 mL standard mouth, crimp cap, chromatography auto-sampler vial, a PDMS membrane and a sorbent, as illustrated in Fig. 2 (the sampler has been recently made commercially available under the name Waterloo Membrane Samplers (WMS) by SiREM, Guelph, ON). The PDMS membrane (Product code: SSP-M823) used in the samplers was procured from Specialty Silicone Products Inc. (Ballston Spa, NY). The membrane had a nominal thickness of 75 μm. The translucent PDMS membrane was supplied with a brown, fiber glass support sheet. The membrane along with the support sheet was first cut to the shape of the top surface of the 2 mL glass vial mouth using a cutting tool. The membrane was then separated from the support and weighed using a microbalance, model MXA 21, from Radwag USA L.L.C. (North Miami Beach, FL). Since the specific gravity of the commercially available PDMS membrane (1.17 ± 0.2) [20] and the area cut by the cutting tool were constant, the weight of the membrane served as a control for the membrane thickness. The thicknesses of the membranes procured were measured at the Department of Mechanical Engineering, University of Water-

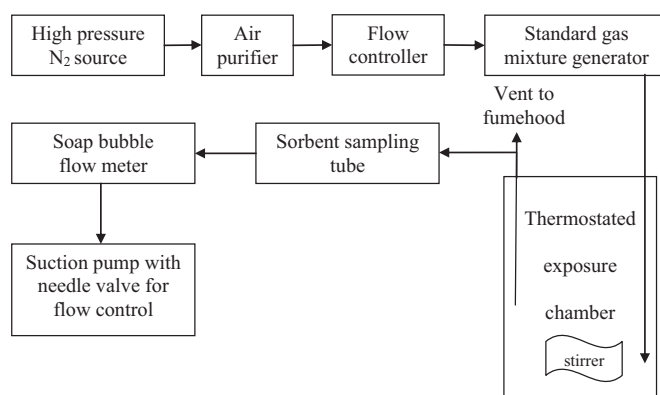


Fig. 3. Schematic of the experimental setup used for the determination of the calibration constants.

loo, using an Olympus U-PMTVC optical microscope (Tokyo, Japan) coupled to a digital image capture system.

Anasorb 747<sup>®</sup>, an activated carbon-based sorbent available commercially in bulk quantities of 100 g from SKC Inc. (Philadelphia, PA), was used as the sorbent for the samplers. Approximately 250 mg of Anasorb 747<sup>®</sup> was weighed into the glass vial and the PDMS membrane was placed on top of the vial. An aluminum cap was then placed on top of the membrane and crimped using a crimper. The rubbery nature of the PDMS membrane provided an air-tight seal between the aluminum cap and the glass vial, which could be verified by warming the vial (either by holding it in the palm of a hand or by blowing hot air on the vial) and watching the membrane bulge. The PDMS membrane is thinner than the PTFE-backed septum accompanying the commercially available aluminum crimp caps. Since this septum was removed before fabrication of the samplers, it required a section of about 1 mm of the rim of the cap to be trimmed before use, in order to crimp with a competent seal. During exposure, the vial was turned upside down so that the sorbent was in contact with the PDMS membrane.

#### 3.3. Experimental setup

The function of the experimental setup was to generate test gas atmospheres with measurable, constant concentrations of the analytes, where the passive samplers could be exposed for specific periods to determine their calibration constants towards the analytes. Schematic diagram of the experimental setup is illustrated in Fig. 3. Nitrogen was passed through an air purifier (containing activated carbon) to remove traces of VOC impurities at a flow rate controlled by a mass flow controller (model MDF-52000LON-OL) purchased from Pneucleus Technologies Inc. (Hollis, NH). The mass flow controller had an operating range of 0–1000 mL/min and was connected to an MKS Instruments (Andover, MA) Type 247 4-channel readout system for setting and monitoring the flow. The purified gas was then passed through a standard gas mixture generator.

The standard gas mixture generator used permeation tubes as the source for analyte vapors. Neat liquid enclosed in these tubes permeated through their walls at a constant rate, and the vapors were swept by purified gas which entered the calibration chamber. The permeation tubes were made from virgin PTFE tubing cut into segments of the desired lengths. The tubes prepared in this way were filled with neat liquids of the test compounds and sealed by means of PTFE plugs and Swagelok<sup>®</sup> ferrules compressed using a custom-made, removable fitting [21]. The PTFE tubes used for the fabrication of the permeation tubes had an outer diameter of 1/4" and a wall thickness of 250 μm. The PTFE plugs were standard, 1/4" diameter rods, which were machined on a lathe to reduce the

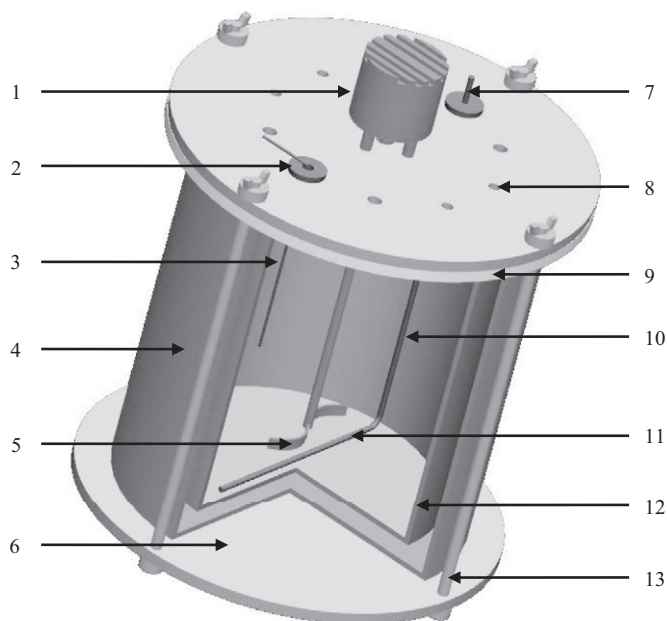


**Fig. 4.** Schematic of the calibration chamber used for the exposure of the TWA-PDMS samplers to standard test gas mixtures. (1) Variable speed motor, (2) vent, (3) tubing for active sampling, (4) jacket, (5) fan blade, (6) aluminum plate, (7) inlet, (8) hole to insert sampler, (9) PTFE plate, (10) gas mixture delivery tube, (11) perforated portion of the tube, (12) glass jar and (13) stainless steel support.

diameter by approximately  $250\ \mu\text{m}$  to tightly fit the tubing. The brass Swagelok<sup>®</sup> ferrules were those used for standard  $1/4''$  outer diameter metal tubing. The permeation tube lengths ranged from 5 cm to 10 cm, depending on the volatility of a compound (longer tubes for less volatile compounds so as to have larger surface area of permeation, and hence increased analyte delivery rate). Depending on the composition of the standard gas mixture required, the respective permeation tubes (each tube containing one neat liquid) were enclosed in a flow-through vessel maintained at a constant temperature by placing it inside a GC oven. Different sets of compounds were thermostated at different temperatures based on the permeation rates of the compounds through PTFE. The outlet of the standard gas mixture generator was connected to the inlet of the calibration chamber, which is detailed next.

The calibration chamber was constructed using a 10-liter cylindrical glass jar (Fig. 4). A PTFE plate of  $1/4''$  thickness was used as the top lid for the glass jar, with an O-ring (made of PTFE-encapsulated Viton, procured from Budlar Inc., Cambridge, ON) between the plate and the jar for sealing. The PTFE plate was held in place with two aluminum plates, one placed on top of the Teflon<sup>®</sup> plate and another below the glass jar and the thermostating jacket. These plates were held together by means of stainless steel rods, threaded on both ends, which were fixed to the bottom and top aluminum plates with the help of nuts. A motor (model Number JB2P021N, Universal Electric Company, MI) was fixed on top of the aluminum plate, and a hole was drilled in the centre of the PTFE and aluminum plates to allow the shaft from the motor to run through this hole. A fan blade made of high-density polyethylene was attached to the bottom of the shaft. The motor itself was connected to a Powerstat<sup>®</sup> variable autotransformer (model 3PN116B, Superior Electric Company, CT) to enable control of the speed of the circulation fan. A segment of  $1/4''$  diameter copper tubing, through which the standard gas mixture entered the chamber, was also passed through the top plates. Holes were drilled in the segment of the inlet tubing

positioned parallel to the bottom of the chamber to allow uniform introduction of the analyte gas mixture. Eight holes were drilled through the top plates (aluminum and PTFE) with diameters small enough to hold the vial-based passive samplers snugly, and the vials were inserted membrane-down during exposure. The whole chamber was placed in a thermostated jacket, the outside of which was insulated by wrapping it with polyester batting. The calibration chamber was maintained at the required temperature throughout the period of sampling by circulating radiator fluid through the jacket with the aid of a circulation thermostat (model number 000-5744, HAAKE, Germany). The  $1/2''$  inner diameter rubber tubing connecting the thermostat and the chamber was also wrapped with the polyester batting insulation. A piece of  $1/8''$  stainless steel tubing inserted into the chamber through the vent was used to draw samples of the chamber atmosphere through sorption tubes for concentration determination.

### 3.4. Determination of LTPRI

An Agilent 6890 GC (Santa Clara, CA) equipped with a split-splitless injector, an FID and an ECD was used for the analysis. The FID was set at  $300\ ^\circ\text{C}$ ; the injector was operated at 1:10 split ratio and maintained at  $275\ ^\circ\text{C}$  with a flow of  $1.2\ \text{mL}/\text{min}$  of helium. The oven was programmed to start at  $35\ ^\circ\text{C}$ , then increased at a rate of  $7\ ^\circ\text{C}$  till it reached  $220\ ^\circ\text{C}$  and was held at  $220\ ^\circ\text{C}$  for 2 min. To correlate the calibration constants to LTPRI, it was necessary to use a capillary column with 100% PDMS stationary phase. The column (RTX-1) was procured from Restek (Bellefonte, PA). For the determination of the LTPRI of aromatic hydrocarbons, a mixture of *n*-alkanes in  $\text{CS}_2$  (from pentane to undecane) was prepared at concentrations of approximately  $100\ \mu\text{g}/\text{mL}$  each in  $\text{CS}_2$ . This solution was used for the determination of the retention times of the *n*-alkanes. Individual solutions of all the aromatic hydrocarbons were also prepared at approximately  $100\ \mu\text{g}/\text{mL}$  in  $\text{CS}_2$  and were used for the determination of the respective analyte's retention times for peak identification. Finally, another solution containing approximately  $100\ \mu\text{g}/\text{mL}$  of all the *n*-alkanes and aromatic hydrocarbons in  $\text{CS}_2$  was prepared. This solution ( $1\ \mu\text{L}$ ) was injected 6 times, and the averages of the retention times of each compound from the 6 injections were used for the calculation of LTPRI. The same method as described above for aromatic hydrocarbons was used for the determination of LTPRI of chlorinated compounds. For the determination of the LTPRI of alcohols and esters, the same methods were used but with a Thermo Electron Corporation Focus GC (Waltham, MA) equipped with a split-splitless injector and an FID and with the same chromatographic conditions as described earlier.

### 3.5. Determination of the calibration constants

The calibration constants were determined using Eq. (4). The knowledge of the extraction efficiency of the analytes from Anasorb 747<sup>®</sup> was required to determine both the analyte mass trapped in the sampler ( $M$ ) and its concentration ( $C_0$ ). Recoveries of all 41 compounds of interest from the Anasorb 747<sup>®</sup> sorbent were determined prior to the exposure experiments. This involved preparation of a stock solution of the respective analytes in  $\text{CS}_2$ , followed by the addition of  $10\ \mu\text{L}$  aliquots of this stock solution to six  $4\ \text{mL}$  vials containing  $250\ \text{mg}$  of Anasorb 747<sup>®</sup> each. The vials were capped and allowed to remain at room temperature for 24 h for equilibration. Even though the extraction efficiency from Anasorb 747<sup>®</sup> was reported to be high for many VOCs using  $\text{CS}_2$  as the desorption solvent, the extraction efficiency could be marginally increased according to the manufacturers specifications by using a polar solvent along with  $\text{CS}_2$  for the extraction. Consequently, isopropyl alcohol (IPA) was used as a cosolvent in proportions depending on the polarity of the analytes studied. For alkanes and aromatic

hydrocarbons, desorption of the analytes from the sorbent was performed by adding 1 mL of CS<sub>2</sub> to each of the six 4 mL vials, followed by shaking intermittently for 30 min. For alcohols, a 50:50 mixture of IPA and CS<sub>2</sub> was used for the extraction. For esters and chlorinated compounds, a 1% solution of IPA in CS<sub>2</sub> was employed. Some of the alcohols had similar retention times under the temperature programming conditions employed. To avoid difficulties imposed by co-elution, the recoveries were determined by analyzing 3-octanol, 2-methyl-1-butanol and 6-methyl-2-heptanol separately from the remaining alcohols listed earlier. The resulting extracts were transferred to 100 µL inserts placed inside 2 mL crimp-top vials, and the analyte amounts were quantified by GC. For the determination of the extraction efficiency of *n*-alkanes and aromatic hydrocarbons, the Agilent 6890 GC was used with the method described earlier. A Thermo Focus GC with Chromquest data acquisition software was used instead of the Agilent GC for quantifying alcohols and esters by gas chromatography using the method described earlier. In the case of chlorinated compounds, desorption was performed using a 1% solution of IPA in CS<sub>2</sub>. Since the retention times of 1,1-dichloroethylene (1,1-DCE) and dichloromethane (DCM) were close with 100% PDMS-based stationary phase capillary columns, a slightly more polar HP-5 stationary phase (95% methyl and 5% phenyl) was used for their separation and quantification. The chromatographic separation and quantification were performed using the method detailed earlier except that the RTX-1 column was replaced with an HP-5 column.

Different sets of standard gas mixtures required for the exposure of the samplers were generated using different sets of permeation tubes. These permeation tubes were placed in a flow-through vessel inside the oven of an HP 5890 GC (with nitrogen flow) one week prior to the exposure experiments to stabilize the permeation rates of the analytes. The permeation tubes with *n*-alkanes, aromatic compounds and alcohols were maintained at 40 °C (±1 °C); the tubes with chlorinated compounds were maintained at 30 °C (±1 °C), and the permeation tubes for esters were maintained at 60 °C (±1 °C) to account for differences in the permeability of PTFE towards each of these classes of compounds. Nitrogen flow rate was set at 800 mL/min (controlled by a mass flow controller). The calibration chamber was maintained at 25 °C ± 1 °C throughout the period of sampling.

The concentration of the analytes in the calibration chamber was measured using sorption tubes by active sampling method. Custom-made sorption tubes (fabricated by the glass blowing shop, University of Waterloo) were loaded with 300 mg of Anasorb 747<sup>®</sup> in the sample section and 100 mg in the back-up section. The sample was drawn from the calibration chamber at a constant rate of approximately 100 mL/min using a suction pump (Model MB-21) procured from Metal Bellows Corp. (Shanon, MA). Flow through the tubes was determined using a soap bubble flow meter, and generally ranged from 80 to 120 mL/min. Analyte concentrations in the calibration chamber were then determined based on the analyte mass trapped by the sorbent tube (determined by gas chromatography) in a given time, and the sample flow rate. The same extraction and chromatographic procedure was followed for the quantification of the analytes trapped by the sorption tubes. The breakthrough layers in the sorption tubes were extracted and analyzed separately. Initial experiments were performed in order to make sure that the sorption capacity of the sorbent was sufficient (so as to not have breakthrough) for the analyte concentrations and standard gas mixture flow rates used in the chamber, yet it was still considered prudent to test the breakthrough layer for confirmation.

The concentration in the chamber was first monitored without the samplers, and the exposure experiments were started when consecutive measurements showed concentrations within ±10% for each analyte. The samplers were then inserted through the sample ports in the calibration chamber, and the start time of the

exposure was recorded. The concentrations of the analytes in the chamber were determined using sorption tubes that were changed every 24–48 h. The concentrations thus obtained were used to calculate the calibration constants of the samplers towards the analytes. After exposure, the samplers were removed from their respective sample ports and the stop time was recorded. Typical exposure durations ranged from 3 to 16 days. After the exposure was completed, the passive samplers were removed and their contents were immediately transferred to separate 4 mL glass vials (along with the PDMS membranes) for extraction and analysis.

To determine the masses of the analytes trapped in the adsorbent medium, the aluminum cap was removed from the sampler with the help of a de-crimper (Chromatographic Specialties Inc., Brockville, ON), and the sorbent along with the PDMS membrane was transferred to a 4 mL vial for desorption (the sorbent tended to stick to the surface of the membrane and it was cumbersome to try to separate it, hence it was decided to extract the membrane along with the sorbent). 1 mL aliquot of the desorption solvent was introduced into the vial, which was then shaken intermittently over 30 min for desorption. After desorption, the vials were centrifuged if necessary, and aliquots of the extract were transferred to 2 mL crimp cap vials with 100 µL inserts for chromatographic analysis. Whenever the approximate analyte masses trapped in the samplers were unknown, the extracts were transferred to two 2 mL vials with 100 µL inserts in them. One of the two vials was used for GC analysis, while the other was reserved for dilution in cases when the concentrations of the analytes exceeded the calibration range of the GC method used. The chromatographic parameters used in the quantification of the compounds trapped by the sorbent in the passive samplers were the same as described in the method for the determination of analyte recoveries.

It should be pointed out that the sampler vial itself can be used for solvent extraction as well as for introduction into the GC autosampler for chromatographic analysis. In this method, the aluminum crimp cap is first be de-crimped and the membrane transferred into the same 2 mL vial. 1 mL of CS<sub>2</sub> is then added to the vial and a new aluminum cap with Teflon<sup>®</sup> lined septum crimped onto it. The advantage of this method is that the vial can be placed directly in the autosampler tray for injection without the need to transfer the sorbent to another vial. Because of the granular nature of the sorbent, no syringe clogging was observed during injection by the chromatographic autosampling/injection systems. In this method, the number of sample preparation steps as well as vials required for extraction was reduced, thereby increasing the throughput. However, no extract could be put aside for dilution in this case.

Experiments reported here were conducted under ideal conditions of good air circulation in the calibration chamber, and hence the calibration constants were dependent only on the permeability of the polymer towards the analytes and the geometry of the membrane, and were independent of the starvation effects. The permeability of PDMS towards various analytes could therefore be determined based on Eq. (3).

## 4. Results and discussion

### 4.1. Analyte recoveries from Anasorb 747<sup>®</sup>

Analyte recoveries from the sorbent were used in the determination of the analyte masses trapped in the sampler, as well as analyte concentrations in the calibration chamber as determined by the active sampling method. The recoveries exceeded 95% in each case for the *n*-alkanes; the lowest recovery among the aromatic hydrocarbons was 93% for propyl benzene. The maximum RSD for both groups of compounds was observed for butyl benzene (2.2%).

Quantitative recovery of polar compounds from Anasorb 747® has always been a problem in the field of air sampling. The recoveries obtained for alcohols were all very high (97–108%), but the reproducibility was not as good as for other groups of analytes, with a maximum RSD of 8.6% for *n*-butanol and a minimum RSD of 3.7% for 2-octanol.

The uncertainty in the recoveries of esters was comparatively low, with a maximum of only 3.3% RSD for butyl acetate. Recoveries of polar alcohols and moderately polar esters were slightly higher than 100% in most cases. This was likely due to complete analyte desorption aided by isopropyl alcohol as a co-solvent and possible slight concentration of the extract, e.g. through sorption of the co-solvent by the sorbent. The recoveries of the chlorinated compounds were all considered to be very good.

#### 4.2. LTPRI of the different groups of model compounds

Table 1 lists the LTPRIs of all compounds used in the study. The retention indices obtained in the laboratory were in close agreement with those reported in the literature [22]. The injection-to-injection retention time precision was less than 0.1% RSD ( $n=6$ ) for all the compounds. LTPRIs can often be determined within  $\pm 5$  units for most chemical species [23,24]. For the purpose of the development of the model reported in this paper, the LTPRI variability of  $\pm 5$  units was considered insignificant.

#### 4.3. Calibration constants and their correlation with LTPRIs

The exposure duration for each of the experiments, the average mass of each analyte trapped in the samplers during exposure in the calibration chamber, as well as the concentrations of the analytes in the calibration chamber are given in Table 1. The calibration constants determined using the samplers equipped with 75  $\mu\text{m}$  thick PDMS membranes and their %RSD values are also reported in Table 1.

The analyte concentrations in the exposure chamber ranged from 0.031  $\text{mg}/\text{m}^3$  to 34.3  $\text{mg}/\text{m}^3$ . Analyte concentrations in the chamber determined in consecutive measurements using sorption tubes over the period of the exposure were within  $\pm 14\%$  of the average value reported in Table 1 for all exposure experiments. Variations in analyte concentrations were generally higher for analytes with higher boiling points in each group. This was likely due to increased sorption capacity of the inside walls and materials of the calibration chamber to heavier analytes. The calibration constants of the samplers towards the 41 model compounds reported here varied between 0.052  $\text{min}/\text{mL}$  for *n*-octanol and 1.223  $\text{min}/\text{mL}$  for 1,1-dichloroethylene. Sampler-to-sampler reproducibility was very good and lower than 10% RSD for all the compounds studied with the exception of 6-methyl-2-heptanol, for which the reproducibility was 12.2% RSD. The reproducibility was exceptionally good for esters, with %RSD values equal to or less than 2.5% for all the analytes. For future field applications, these variations can be considered minimal and errors arising from them negligible when compared to other factors involved in field studies.

The calibration constants of the TWA-PDMS samplers toward *n*-alkanes decreased exponentially from 0.765  $\text{min}/\text{mL}$  for *n*-hexane to 0.074  $\text{min}/\text{mL}$  for *n*-decane. Since the calibration constants were inversely proportional to the permeability of PDMS towards the analytes, this trend indicated an exponential increase in the permeability of PDMS from *n*-hexane to *n*-decane as indicated in Table 1. This is in agreement with data on permeability of PDMS towards *n*-alkanes published in the literature and discussed in Section 2. A plot of  $\ln(k)$  vs. LTPRI for *n*-alkanes, depicted in Fig. 5(a), showed a straight line correlation with an excellent correlation coefficient of 0.9976. This supported the hypothesis that the calibration con-

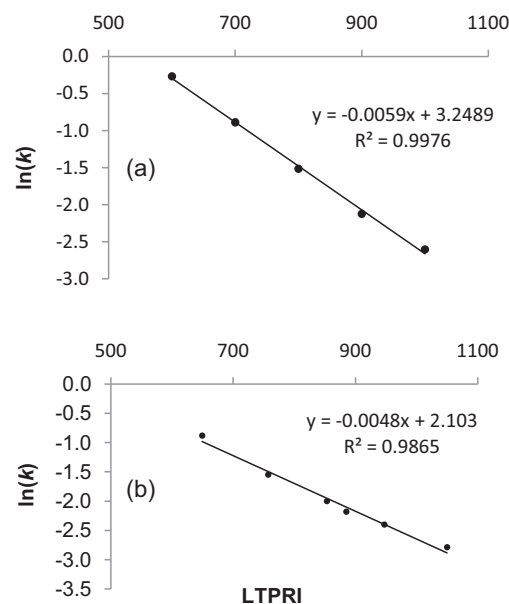


Fig. 5. (a)  $\ln(k)$  vs. LTPRI correlation for aromatic hydrocarbons and (b)  $\ln(k)$  vs. LTPRI correlation for *n*-alkanes.

stants of the samplers were mainly determined by the analyte partition coefficients between the PDMS membrane and air (hence they were correlated to LTPRI), as discussed in Section 2 of this paper.

The results confirmed the important reasons for the discrepancy observed between the results presented here and by Zabiegała et al. Firstly, the thickness of the membrane used earlier (50  $\mu\text{m}$ ) was different from that used by the author (75  $\mu\text{m}$ ) and the degree of polymer cross-linking could also be different. Further, in the exposure chamber used by Zabiegała et al. there was no forced air circulation. The absence of proper air circulation introduces starvation effects and this would affect the uptake rates of the samplers towards various analytes to a different extent. Finally, discerning a logarithmic curve is easier when the data spans several orders of magnitude. The calibration constants obtained by Zabiegała et al. (e.g. for *n*-alkanes) were within 2 orders of magnitude (0.230  $\text{min}/\text{mL}$  for *n*-hexane and 0.064  $\text{min}/\text{mL}$  for *n*-decane) and determining the relationship between  $k$  and LTPRI was further challenging because of the uncertainties in the determination of the calibration constants.

The calibration constants of the samplers towards aromatic hydrocarbons indicated a similar trend of exponential decrease from 0.414  $\text{min}/\text{mL}$  for benzene to 0.061  $\text{min}/\text{mL}$  for butyl benzene. Boscani and co-workers determined the permeability of benzene, toluene, ethyl benzene and propyl benzene using membrane inlet mass spectrometry, and found the same exponential increase in the permeability of PDMS from benzene through propyl benzene [25]. Similarly to *n*-alkanes, the linear correlation between  $\ln(k)$  and LTPRI for aromatic hydrocarbons (as shown in Fig. 5(b)) supported the hypothesis that the calibration constants were mainly a function of partition coefficients of the analytes.

The analytes in the alcohol group were either primary or secondary alcohols, and had either linear or branched alkyl chains in them. The calibration constants of the samplers towards *n*-alcohols from *n*-butanol to *n*-octanol showed a trend similar to those observed for *n*-alkanes and aromatic hydrocarbons, i.e. an exponential decrease in the calibration constants and consequently a linear correlation between  $\ln(k)$  and LTPRI, with a correlation coefficient of 0.9903 (as shown in Fig. 6). This correlation was again due to the dominant nature of partitioning in permeation

**Table 1**  
Calibration constants at 25 °C ( $\pm 1$  °C);  $k$  is the average calibration constant observed when  $n$  passive samplers were employed during the exposure to the indicated set of compounds.

Analyte	LTPRI	Exposure duration (min)	Average mass in $n$ samplers ( $\mu\text{g}$ )	Concentration in the chamber ( $\text{mg}/\text{m}^3$ )	$k$ (min/mL)	$n$	% RSD	Permeability ( $\text{cm}^2 \text{min}^{-1}$ )
Hexane	600	5354	10.2	1.46	0.765	5	7.3	0.041
Heptane	700	5354	12.0	0.919	0.411	5	9.4	0.077
Octane	800	5354	11.5	0.473	0.220	5	9.4	0.144
Nonane	900	5354	9.9	0.219	0.119	5	7.8	0.265
Decane	1000	5354	8.5	0.117	0.074	5	8.7	0.428
Benzene	649	5354	17.4	1.35	0.414	5	7.3	0.076
Toluene	757	5354	33.7	1.33	0.213	5	7.9	0.149
Ethyl benzene	853	5354	21.4	0.538	0.135	5	7.8	0.234
<i>o</i> -Xylene	885	5354	11.3	0.238	0.113	5	6.8	0.280
Propyl benzene	947	5354	17.8	0.300	0.090	5	7.0	0.350
Butyl benzene	1050	5354	12.2	0.139	0.061	5	8.5	0.516
2-Methyl-1-propanol	609	16160	3.01	0.147	0.788	7	6.4	0.040
<i>n</i> -Butanol	643	16160	11.1	0.351	0.512	7	6.6	0.062
2,3-Dimethyl-2-butanol	719	16160	2.27	0.077	0.549	7	6.0	0.058
<i>n</i> -Pentanol	748	16160	14.6	0.232	0.258	7	5.3	0.123
2-Hexanol	782	16160	13.4	0.189	0.228	7	5.0	0.139
2,4-Dimethyl-3-pentanol	827	16160	5.51	0.086	0.253	7	6.1	0.125
<i>n</i> -Hexanol	850	16160	15.3	0.131	0.138	7	5.5	0.229
<i>n</i> -Heptanol	952	16160	16.5	0.077	0.075	7	4.8	0.419
2-Octanol	985	16160	19.3	0.082	0.069	7	5.0	0.461
2-Ethyl-1-hexanol	1016	16160	7.83	0.031	0.064	7	6.1	0.493
<i>n</i> -Octanol	1055	16160	13.3	0.043	0.052	7	6.7	0.605
2-Methyl-1-butanol	720	22950	5.77	0.101	0.404	5	7.6	0.078
3-Octanol	983	22950	9.46	0.049	0.120	5	9.7	0.264
6-Methyl-2-heptanol	952	22950	23.4	0.096	0.095	5	12.2	0.333
Ethyl acetate	594	11628	218.4	14.2	0.754	7	2.5	0.042
Propyl acetate	693	11628	168.1	5.75	0.398	7	2.5	0.080
Methyl butyrate	703	11628	218.1	6.84	0.365	7	2.5	0.087
Sec-butyl acetate	740	11628	34.1	1.15	0.392	7	2.4	0.081
Ethyl butyrate	780	11628	176.6	3.36	0.221	7	2.4	0.143
Butyl acetate	792	11628	169.6	2.95	0.202	7	2.0	0.156
Propyl butyrate	878	11628	151.1	1.66	0.128	7	2.0	0.248
Butyl butyrate	976	11628	134	0.927	0.081	7	2.4	0.392
1,1-Dichloroethylene	508	2925	82.3	34.3	1.223	5	5.1	0.026
Dichloromethane	510	2925	64.5	18.1	0.824	5	5.8	0.038
<i>cis</i> -1,2-Dichloroethylene	592	2925	32.6	5.82	0.524	5	5.6	0.060
Chloroform	603	2925	26.1	4.58	0.514	5	5.1	0.062
1,1,1-Trichloroethane	625	2925	2.98	0.800	0.787	5	6.0	0.040
1,2-Dichloroethane	633	2925	24.3	3.22	0.388	5	5.4	0.082
Carbontetrachloride	655	2925	6.76	1.54	0.667	5	6.1	0.047
Trichloroethylene	696	2925	120.5	12.5	0.305	5	7.1	0.104

through PDMS. Even though there was also a linear correlation for the  $\ln(k)$  vs. LTPRI relationship for the alcohols with branched alkyl groups and secondary alcohols, the spread in the data points was much higher than for  $n$ -alcohols. This indicated that branching of the side chains and/or the nature of the alcohol (primary or secondary) played important roles in determining the permeability of PDMS towards these analytes, and consequently in determining the calibration constants.

A decrease in the permeability was observed between primary alcohols and the corresponding secondary alcohols with the

–OH group in the 2 position. For example, the calibration constant of  $n$ -hexanol was 0.138 min/mL, while that for 2-hexanol was 0.228 min/mL. Similarly, the calibration constant of  $n$ -octanol was 0.052 min/mL, while that for 2-octanol was 0.069 min/mL. The decrease in permeability can be explained based on the mechanism of the partitioning process. When a molecule dissolves in the liquid polymer matrix, energy is required to disrupt the intermolecular attractions holding the individual PDMS chains together. Some of this energy is regained as a result of interactions between the analyte molecule and the PDMS matrix. The lower the energy cost of dissolution, the higher the tendency for the analyte molecule to partition into PDMS. One of the important factors affecting the energy of dissolution of a molecule is its hydrophobic surface area. The larger it is, the stronger the interaction between the analyte molecule and the hydrophobic PDMS chains. With linear alcohols such as  $n$ -hexanol, the long hydrophobic chains can align with the PDMS chains for maximum interaction. In the case of secondary alcohols, the hydrophobic surface area is reduced because of the geometric positioning of the –OH groups, thereby reducing the intermolecular attractions when compared to that for  $n$ -alcohols. Consequently, the partition coefficients for  $n$ -alcohols are greater than those for the corresponding 2-alkanols. Further, the diffusion coefficients of  $n$ -alcohols are higher compared to those of the corresponding 2-alkanols due to the smaller “minimum cross section” of the former compared to the latter [26]. A similar observation was

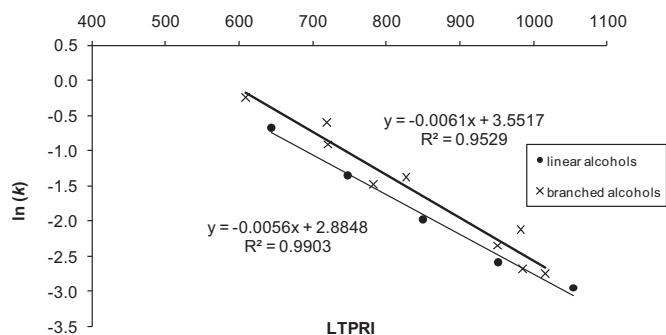


**Fig. 6.**  $\ln(k)$  vs. LTPRI correlation for alcohols.



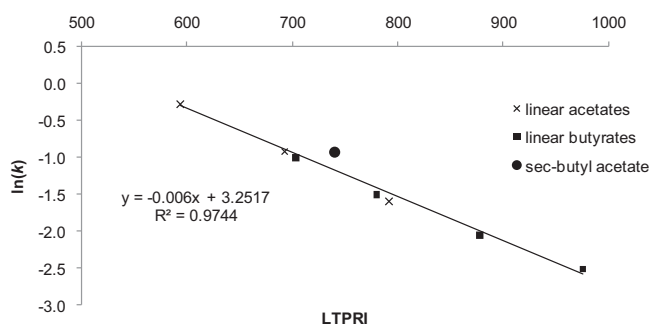


Fig. 7.  $\ln(k)$  vs. LTPRI correlation for esters.

made by Favre et al., who found that the diffusion coefficient of *n*-butanol in PDMS ( $3.11 \times 10^{-10} \text{ m}^2 \text{ s}^{-1}$ ) was higher than that for *s*-butanol ( $2.25 \times 10^{-10} \text{ m}^2 \text{ s}^{-1}$ ) and *t*-butanol ( $2.66 \times 10^{-10} \text{ m}^2 \text{ s}^{-1}$ ) [27].

Branching in the alkyl chain of alcohol molecules resulted in a decrease in the permeability through PDMS. For example, permeability of PDMS towards 2-methyl-1-butanol ( $k = 0.404 \text{ min/mL}$ ) was lower than that for *n*-pentanol ( $k = 0.258 \text{ min/mL}$ ). Similarly, the permeability of 2-methyl-1-propanol in PDMS ( $k = 0.788$ ) was lower than that for *n*-butanol ( $k = 0.512$ ). This can be explained based on arguments similar to those presented for the difference in permeability between primary and secondary alcohols above. Since branching reduces the hydrophobic surface area of a molecule, the partition coefficients of compounds with branched alkyl chains are smaller than those with linear alkyl chains. Further, branching increases the minimum cross section of the molecules, thereby decreasing their diffusion coefficients. When considering all the alcohols together, there was still a linear trend with a correlation coefficient of 0.9437. In general, it could be concluded that the trends for homologous groups of the highly polar alcohols were similar to those observed for the highly non-polar alkanes and aromatic hydrocarbons.

Esters have polarities ranging between those of *n*-alkanes and alcohols. As anticipated, there was a very good linear correlation between  $\ln(k)$  and LTPRI (Fig. 7) for the two homologous ester series, the acetates and the butyrates. Similarly to the trends observed for the alcohols, PDMS had lower permeability for *sec*-butyl acetate ( $k = 0.392 \text{ min/mL}$ ) when compared to that for butyl acetate ( $0.202 \text{ min/mL}$ ), which could be explained by the differences in the partition coefficients of the two compounds and the lower diffusion coefficient of *sec*-butyl acetate in PDMS due to steric hindrance caused by branching.

The trend in the calibration constants of DCM, chloroform, and carbon tetrachloride seemed at first counter-intuitive. Since the retention indices of these three compounds increase with the increase in the number of chlorine atoms in the molecule, the calibration constants were expected to decrease accordingly from DCM to carbon tetrachloride. However, the average calibration constant for carbon tetrachloride ( $0.667 \text{ min/mL}$ ) was significantly greater than that for chloroform ( $0.514 \text{ min/mL}$ ). A subsequent literature search indicated that the diffusion coefficients of these three compounds in PDMS play an important role in determining the net permeability of the molecules through this polymer [28]. Even though the partition coefficients increase with the increase in the number of chlorine atoms, it is evident from the results that the decrease in the diffusion coefficients with the increase in the number of chlorine atoms (and hence the molecular weight) plays a much more important role for these compounds compared with the remaining analytes. The significant role of the diffusion coefficients can be explained based on the molecular weights of these analytes (84.93 for dichloromethane,

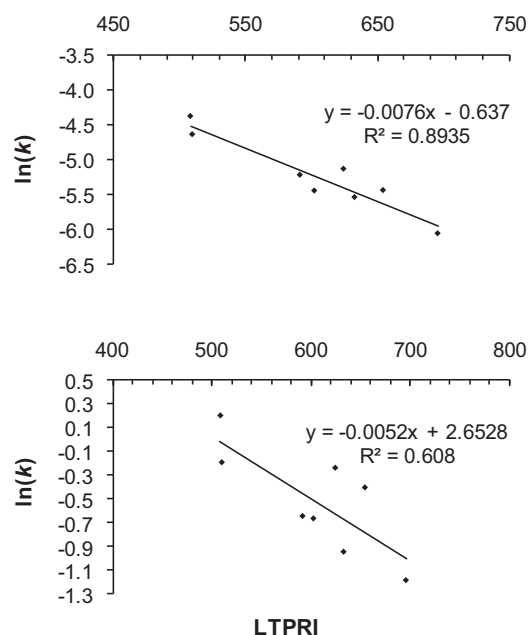


Fig. 8. (a)  $\ln(k/MW)$  vs. LTPRI correlation for chlorinated compounds and (b)  $\ln(k)$  vs. LTPRI correlation for chlorinated compounds.

119.38 for chloroform, and 153.82 for carbon tetrachloride), which change much more from one compound to another in the homologous series than for the *n*-alkanes and aromatic hydrocarbons. Dotremont et al. also reported that the diffusion coefficients decreased in the order  $\text{CH}_2\text{Cl}_2 > \text{CHCl}_3 > \text{CCl}_4$ , while partition coefficients decreased in the order  $\text{CCl}_4 > \text{CHCl}_3 > \text{CH}_2\text{Cl}_2$ , but because of their relative magnitudes, the permeability decreased in the order  $\text{CHCl}_3 > \text{CCl}_4 > \text{CH}_2\text{Cl}_2$  [29]. A similar observation can also be made for the calibration constant of 1,1,1-TCA, which has a higher LTPRI than *cis*-DCE and chloroform, but has a larger calibration constant than these two compounds.

As a consequence of the deviation from the general trend observed for other groups of compounds, the  $\ln(k)$  vs. LTPRI relationship for chlorinated compounds showed a significantly worse correlation coefficient of 0.6080 (Fig. 8(a)). Further, the low value of the correlation coefficient indicated that alternative correlations should be considered (Case 2 described in Section 2). The diffusivity of a molecule in PDMS is inversely proportional to its molecular weight, which spans a wide range for the chlorinated compounds. Using this assumption a better correlation coefficient of 0.8938 was obtained by plotting LTPRI against  $\ln(k/MW)$ , as shown in Fig. 8(b).

The correlation coefficient for the relationship between  $\ln(k)$  and LTPRI for all 41 compounds studied was 0.9475 (Fig. 9). The  $\ln(k/MW)$  vs. LTPRI correlations were also examined for the indi-

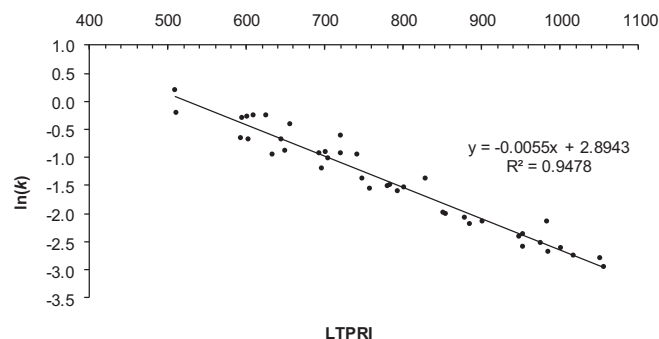


Fig. 9.  $\ln(k)$  vs. LTPRI correlation for all 41 compounds studied.

**Table 2**  
Correlation coefficients and regression line equations for the calibration constants at 25 °C ( $\pm 1$  °C) for different classes of compounds.

Compound class	Parameter	LTPRI vs. $\ln(k)$	LTPRI vs. $\ln(k/MW)$
<i>n</i> -Alkanes	Correlation coefficient Equation	0.9976 $\ln(k) = -0.0059 \times \text{LTPRI} + 3.2489$	0.9936 $\ln(k/MW) = -0.007 \times \text{LTPRI} - 0.6218$
Aromatic hydrocarbons	Correlation coefficient Equation	0.9865 $\ln(k) = -0.0048 \times \text{LTPRI} + 2.103$	0.9903 $\ln(k/MW) = -0.0061 \times \text{LTPRI} - 1.3874$
Alcohols	Correlation coefficient Equation	0.9437 $\ln(k) = -0.006 \times \text{LTPRI} + 3.3192$	0.9729 $\ln(k/MW) = -0.0073 \times \text{LTPRI} - 0.2132$
Esters	Correlation coefficient Equation	0.9744 $\ln(k) = -0.006 \times \text{LTPRI} + 3.2517$	0.9865 $\ln(k/MW) = -0.0073 \times \text{LTPRI} - 0.4933$
Chlorinated compounds	Correlation coefficient Equation	0.6080 $\ln(k) = -0.0052 \times \text{LTPRI} + 2.6528$	0.8934 $\ln(k/MW) = -0.0076 \times \text{LTPRI} - 0.6371$
Overall correlation for LTPRI vs. $\ln(k/MW)$	Correlation coefficient/Equation	0.9502/ $\ln(k/MW) = -0.0063 \times \text{LTPRI} - 1.1979$	
Overall correlation for LTPRI vs. $\ln(k)$	Correlation coefficient/Equation	0.9475/ $\ln(k) = -0.0055 \times \text{LTPRI} + 2.9049$	

vidual classes of compounds, as well as all compounds put together and the correlation equations and the respective correlation coefficients are presented in Table 2. The correlation equations and correlation coefficients alone cannot determine if one method of estimation is better than the other, hence statistical analysis of the residuals was performed to determine if there were any significant differences between the experimentally determined calibration constants and the various estimated calibration constants.

#### 4.4. Statistical analysis of the $\ln(k)$ vs. LTPRI and $\ln(k/MW)$ vs. LTPRI correlations

Statistical analysis was performed to determine if there were any significant differences between the various methods used for estimating the calibration constants. Two-tailed, paired Student's *t* test was employed for this purpose. The significance of the differences was determined at the 95% confidence level by comparing the calculated *t* value with that of the critical (two tail) value for the respective number of paired observations (*n*) [30]. The experimentally determined calibration constants and the estimated calibration constants using different methods are listed in Table 3. The results from the statistical tests are summarized in Table 4.

When the experimentally determined calibration constants ( $k_{\text{exp}}$ ) were compared separately with each of the four sets of estimated calibration constants ( $k_{\text{est}}$ ) for all 41 compounds studied (*n* = 41), no significant differences between the values obtained using the different estimation methods and the experimental values were observed in any of the cases. The statistical tests also found no significant differences between the  $k_{\text{est}}$  values obtained from the class-specific  $\ln(k)$  vs. LTPRI correlations and class-specific  $\ln(k/MW)$  vs. LTPRI correlation, as well as between overall  $\ln(k)$  vs. LTPRI and overall  $\ln(k/MW)$  vs. LTPRI correlations.

The maximum difference between the  $k_{\text{exp}}$  and the  $k_{\text{est}}$  obtained using the overall  $\ln(k)$  vs. LTPRI correlation was 43.2% (1,2-dichloroethane). Analysis of the residuals in this case showed that out of the 41 compounds studied, the calibration constants for 14 of them could be estimated within  $\pm 10\%$ , 26 within  $\pm 20\%$ , 37 within  $\pm 30\%$  and all the 41 compounds within  $\pm 50\%$ . Considering that the identity of a compound does not have to be known at the time of sampling and analysis when using the  $\ln(k)$  vs. LTPRI correlation, the error related to the estimation of the calibration constants could be considered fairly low.

Using the overall  $\ln(k/MW)$  vs. LTPRI correlations resulted in maximum differences of 23.2% for alkanes,  $-12.4\%$  for aromatic hydrocarbons, 40.0% for alcohols,  $-20.5\%$  for esters, and  $-60.0\%$  for the chlorinated hydrocarbons. Even though the correlation coef-

ficients for the  $\ln(k/MW)$  vs. LTPRI relationship were higher, the statistical analysis indicated that the estimated calibration constants were not necessarily more accurate than those obtained with the overall  $\ln(k)$  vs. LTPRI correlation.

The maximum differences between the  $k_{\text{exp}}$  and the  $k_{\text{est}}$  obtained using class specific  $\ln(k)$  vs. LTPRI correlation were  $-6.8\%$  for alkanes, 13.5% for aromatic hydrocarbons, 36.7% for alcohols, 22.4% for esters, and  $-36.0\%$  for chlorinated hydrocarbons. The maximum differences between  $k_{\text{exp}}$  and  $k_{\text{est}}$  obtained using class-specific  $\ln(k/MW)$  vs. LTPRI correlations were 22.8% for *n*-alkanes, 10.3% for aromatic hydrocarbons, 36.9% for alcohols, 18.6% for esters, and  $-26.1\%$  for chlorinated hydrocarbons.

Statistical comparisons of  $k_{\text{exp}}$  values with the four sets of  $k_{\text{est}}$  values (Table 4) were also performed separately by considering the individual groups of analytes (*n* = 5, 6, 14, 8, and 8 for *n*-alkanes, aromatic hydrocarbons, alcohols, esters and chlorinated compounds, respectively). The tests indicated no significant differences between the respective pairs of methods for *n*-alkanes and esters. In the case of chlorinated compounds, the tests indicated that there were no significant differences between the experimental values and the estimates obtained using the different methods with the exception of the  $k_{\text{est}}$  values obtained using the  $\ln(k)$  vs. LTPRI correlation. On the other hand, for alcohols a significant difference was observed between the  $k_{\text{exp}}$  values and the  $k_{\text{est}}$  values obtained from the overall  $\ln(k/MW)$  vs. LTPRI correlation. In this case, the structure of the individual linear and branched alcohols played an important role in deciding both the partition coefficients and the diffusion coefficients in PDMS, as discussed earlier. Consequently, corrections for the molecular weight did not account for the observed variations in permeability of alcohols through PDMS.

In the case of aromatic hydrocarbons, the calibration constants for all the individual analytes obtained using class specific  $\ln(k/MW)$  vs. LTPRI correlation were consistently higher than those obtained using the class specific  $\ln(k)$  vs. LTPRI correlation. Consequently, the test showed significant differences between the two methods used for estimating the calibration constants. For *n*-alkanes and esters, there were no significant differences between  $k_{\text{est}}$  values obtained from the class-specific  $\ln(k)$  vs. LTPRI correlations and the class-specific  $\ln(k/MW)$  vs. LTPRI correlations, as well as between  $k_{\text{est}}$  values obtained from the overall  $\ln(k)$  vs. LTPRI correlation and the overall  $\ln(k/MW)$  vs. LTPRI correlation. In general, even though the correlation coefficients were consistently higher for the correlations obtained for all classes of compounds using the  $\ln(k/MW)$  vs. LTPRI relationship, analysis of the residuals showed no significant improvement in the accuracy of the estimation of the calibration constants except for the chlorinated compounds.

**Table 3**  
Analysis of the residuals (difference between actual and estimated calibration constants) for class-specific and non-class-specific correlations.

	Class-specific $k_{\text{est}}$ using LTPRI vs. $\ln(k)$ correlation	% Diff. from $k_{\text{exp}}$	Class-specific $k_{\text{est}}$ using LTPRI vs. $\ln(k/MW)$ correlation	% Diff. from $k_{\text{exp}}$	$k_{\text{est}}$ using LTPRI vs. $\ln(k)$ correlation for all compounds studied	% Diff. from $k_{\text{exp}}$	$k_{\text{est}}$ using LTPRI vs. $\ln(k/MW)$ correlation for all compounds studied	% Diff. from $k_{\text{exp}}$
<i>n</i> -Hexane	0.747	2.2	0.615	19.5	0.667	12.8	0.587	23.2
<i>n</i> -Heptane	0.414	-0.7	0.348	15.3	0.385	6.5	0.364	11.6
<i>n</i> -Octane	0.230	-4.6	0.193	12.0	0.222	-1.0	0.221	-0.5
<i>n</i> -Nonane	0.127	-6.8	0.106	11.4	0.128	-7.4	0.132	-10.8
<i>n</i> -Decane	0.071	4.5	0.057	22.8	0.074	0.0	0.078	-5.6
Benzene	0.363	12.4	0.372	10.3	0.508	-22.7	0.390	5.8
Toluene	0.216	-1.7	0.227	-6.8	0.281	-32.1	0.233	-9.8
Ethyl benzene	0.136	-0.9	0.146	-7.7	0.166	-22.5	0.147	-8.6
<i>o</i> -Xylene	0.117	-3.6	0.120	-6.1	0.139	-23.0	0.120	-6.3
Propyl benzene	0.087	4.0	0.093	-2.7	0.099	-9.1	0.092	-1.6
Butyl benzene	0.053	13.5	0.055	9.6	0.056	8.5	0.054	12.4
2-Methyl-1-propanol	0.717	9.0	0.712	9.7	0.635	19.4	0.478	39.3
<i>n</i> -Butanol	0.582	-13.7	0.551	-7.6	0.525	-2.6	0.385	24.9
2,3-dimethyl-2-butanol	0.370	32.6	0.434	20.9	0.347	36.9	0.329	40.0
<i>n</i> -Pentanol	0.311	-20.6	0.303	-17.3	0.296	-14.6	0.237	8.2
2-Hexanol	0.253	-10.9	0.271	-19.1	0.244	-7.3	0.221	3.1
2,4-Dimethyl-3-pentanol	0.193	23.6	0.222	12.4	0.191	24.5	0.189	25.2
<i>n</i> -Hexanol	0.169	-21.9	0.165	-19.1	0.169	-21.9	0.144	-4.3
<i>n</i> -Heptanol	0.091	-20.8	0.088	-16.3	0.096	-27.2	0.086	-14.0
2-Octanol	0.075	-9.0	0.077	-12.3	0.080	-16.6	0.078	-14.1
2-Ethyl-1-hexanol	0.062	3.2	0.061	4.5	0.068	-5.2	0.064	-0.4
<i>n</i> -Octanol	0.049	5.6	0.046	11.8	0.055	-4.6	0.051	3.2
2-Methyl-1-butanol	0.367	9.2	0.370	8.3	0.344	14.9	0.281	30.3
3-Octanol	0.076	36.7	0.078	34.6	0.081	32.4	0.079	33.7
6-Methyl-2-heptanol	0.092	3.7	0.099	-4.0	0.096	-1.3	0.097	-1.9
Ethyl acetate	0.732	2.9	0.704	6.6	0.689	8.6	0.624	17.3
Propyl acetate	0.405	-1.8	0.398	0.1	0.401	-0.7	0.389	2.3
Methyl butyrate	0.380	-4.1	0.367	-0.7	0.377	-3.5	0.363	0.5
Sec-butyl acetate	0.304	22.4	0.319	18.6	0.308	21.4	0.327	16.5
Ethyl butyrate	0.240	-8.5	0.239	-8.1	0.248	-12.0	0.255	-15.3
Butyl acetate	0.223	-10.4	0.219	-8.2	0.232	-14.7	0.236	-16.9
Propyl butyrate	0.133	-4.2	0.131	-2.4	0.145	-13.1	0.154	-20.5
Butyl butyrate	0.074	8.2	0.071	11.9	0.084	-4.6	0.092	-14.3
1,1-Dichloroethylene	1.009	17.5	1.076	12.0	1.103	9.8	1.176	3.8
Dichloromethane	1.001	-21.5	0.932	-13.1	1.094	-32.8	1.021	-23.9
<i>cis</i> -1,2-Dichloroethylene	0.655	-25.0	0.572	-9.1	0.698	-33.2	0.697	-33.0
Chloroform	0.619	-20.4	0.648	-26.1	0.657	-27.9	0.801	-55.9
1,1,1-Trichloroethane	0.551	29.9	0.612	22.2	0.582	26.0	0.778	1.1
1,2-Dichloroethane	0.528	-36.0	0.426	-9.7	0.556	-43.2	0.548	-41.1
Carbontetrachloride	0.472	29.3	0.562	15.8	0.493	26.0	0.743	-11.4
Trichloroethylene	0.380	-24.5	0.350	-14.6	0.393	-28.6	0.489	-60.0

$k_{\text{exp}}$  is the experimentally obtained calibration constant, and  $k_{\text{est}}$  is the calibration constant estimated using the correlations specified in the Table.

#### 4.5. Application of the calibration constant – LTPRI relations for the analysis of unknown samples

Determining analyte concentration over a specific time period by passive sampling requires the knowledge of two parameters: the calibration constant and the chromatographic response factor for the analyte. If the calibration constant is not known, it can be estimated based on the class-specific correlation or the overall correlation (depending on whether the identity of the analyte can be determined, e.g. using mass spectrometry). If the identity of the analyte is established after the analysis of the samplers, the chromatographic detector can be calibrated for that specific analyte; on the other hand, if the analyte identity cannot be established, a flame ionization detector can be used based on the assumption that the response factor for the unknown analyte is similar to that of a standard such as benzene or toluene. Using the estimated calibration constant based on the overall correlation between  $\ln(k)$  and LTPRI with an FID as a detector for GC can then be a powerful technique to estimate parameters such as Total Petroleum Hydrocarbons (TPH) in vapor phase. Such an approach to the determination of TPH is not possible with diffusive-type passive samplers.

The detection limits of the sampler towards an analyte depend on the uptake rate, deployment period and the detection limits

of the chromatographic method used. In this project, quantitative analysis of analytes in the extracts ( $\text{CS}_2$  for some and  $\text{CS}_2$  + isopropyl alcohol for others) was performed using GC-FID and GC-ECD, depending on the application. Analyte concentrations in the standard test gas atmosphere were deliberately fixed at high levels in order to meet the quantitation limits of the detectors. However, the same analysis could be performed using a GC-MS system, which could further improve the sensitivity for many of the compounds presented in the manuscript. Nevertheless, even in the configuration used in the study sensitivity was acceptable. For example, a quantitation limit of 50 ng/mL (in carbon disulphide) was easily achieved for most of the compounds listed under EPA method TO-14 with splitless injection of 1  $\mu\text{L}$  of the extract into the GC. For benzene, this corresponded to a quantitation limit of 17  $\mu\text{g}/\text{m}^3$  for a 1 day deployment, and 2.4  $\mu\text{g}/\text{m}^3$  for a one week deployment. The quantitation limits could be further reduced by one order of magnitude when using large volume injection of 10  $\mu\text{L}$  of the extract, and by two to three orders of magnitude by replacing the currently used sorbent with a thermally desorbable one. The results of these experiments will be described in an upcoming publication.

It is also important to note that as the volatility decreases, the PDMS membrane might absorb large amounts of the analyte at steady state. However, since the sorbent keeps the gas phase con-

**Table 4**  
Results of two-tailed, paired, Student's *t* test employed to determine the significance of the difference between various methods used to estimate the calibration constant at the 95% confidence level.

Analytes	Variable 1 →	$k_{\text{exp}}$	$k_{\text{exp}}$	$k_{\text{exp}}$	$k_{\text{exp}}$	$k_{\text{est}}$ using class specific LTPRI vs. $\ln(k)$ correlation	$k_{\text{est}}$ using overall LTPRI vs. $\ln(k)$ correlation
	Variable 2 →	$k_{\text{est}}$ using class specific LTPRI vs. $\ln(k)$ correlation	$k_{\text{est}}$ using class specific LTPRI vs. $\ln(k/MW)$ correlation	$k_{\text{est}}$ using overall – LTPRI vs. $\ln(k)$ correlation	$k_{\text{est}}$ using overall LTPRI vs. $\ln(k/MW)$ correlation	$k_{\text{est}}$ using class specific LTPRI vs. $\ln(k)$ correlation	$k_{\text{est}}$ using overall LTPRI vs. $\ln(k/MW)$ correlation
All compounds ( <i>n</i> = 41)	Significance	NS	NS	NS	NS	NS	NS
	<i>t</i> Stat	0.59	1.39	0.67	−0.42	0.89	−1.39
	<i>t</i> Critical two-tail	2.02	2.02	2.02	2.02	2.02	2.02
<i>n</i> -Alkanes ( <i>n</i> = 5)	Significance	NS	NS	NS	NS	NS	NS
	<i>t</i> Stat	−0.03	2.12	1.38	0.98	2.51	0.06
	<i>t</i> Critical two-tail	2.78	2.78	2.78	2.78	2.78	2.78
Aromatic hydrocarbons ( <i>n</i> = 6)	Significance	NS	NS	NS	NS	S	NS
	<i>t</i> Stat	1.04	0.28	−2.31	−1.21	−4.68	1.66
	<i>t</i> Critical two-tail	2.57	2.57	2.57	2.57	2.57	2.57
Alcohols ( <i>n</i> = 14)	Significance	NS	NS	NS	S	NS	NS
	<i>t</i> Stat	0.85	0.74	1.71	2.25	−0.87	1.97
	<i>t</i> Critical two-tail	2.16	2.16	2.16	2.16	2.16	2.16
Esters ( <i>n</i> = 8)	Significance	NS	NS	NS	NS	NS	NS
	<i>t</i> Stat	0.48	1.00	1.00	0.14	1.28	−2.19
	<i>t</i> Critical two-tail	2.36	2.36	2.36	2.36	2.36	2.36
Chlorinated compounds ( <i>n</i> = 8)	Significance	NS	NS	S	NS	NS	S
	<i>t</i> Stat	0.03	0.16	−3.52	−0.35	0.18	−3.97
	<i>t</i> Critical two-tail	2.36	2.36	2.36	2.36	2.36	2.36

"S" indicates a significant difference and "NS" indicates no significant difference between the two sets of data (variable 1 and variable 2) for the respective group of analytes and corresponding *n* values. "*t* Stat" indicates the calculated *t* value for the data and "*t* critical two-tail" indicates the tabulated *t* value at 95% confidence interval.

centration of the analyte inside the vial at practically zero, the rate of migration of the analyte through the membrane should never be zero. This has been tested for naphthalene and found to be true. On the other hand, for analytes with very large partition coefficients the membrane might not act as the uptake rate-limiting barrier, which makes quantitative analysis difficult. This makes the sampler suitable for quantitative analysis of volatile compounds only, and that is the application for which it is intended. Any results obtained for semi-volatile compounds should be treated as estimates only, especially that the samplers have not been properly characterized for such applications.

## 5. Conclusions

This paper introduced a new permeation passive sampler which is inexpensive, easy to fabricate and use. It utilizes PDMS properties such as high permeability towards VOCs and low permeability towards moisture. Reproducibilities of the extraction efficiencies and the calibration constants were generally very good for consideration in field applications, and such applications will be presented in upcoming papers.

The approach proposed in this paper allows easy and fast estimation of the calibration constants of permeation passive samplers equipped with PDMS membranes. Using LTPRI for the estimation of the calibration constants comes with the advantage that the compound's identity does not need to be known at the time of sampling. Consequently, total petroleum hydrocarbon concentrations can be easily estimated using the correlation between LTPRI and the calibration constants. The knowledge of PDMS permeability towards various analytes presented in this paper should be valuable for the development of related analytical techniques such as membrane inlet mass spectrometry (MIMS) and membrane extraction with a sorbent interface (MESI) [31,32].

Owing to the hydrophobic nature of PDMS, application of the samplers in soil gas environments with high humidity is possible. Studies on the effect of humidity and temperature on the uptake rate of the samplers are presented in the second part of the paper, and that on the membrane geometry will be presented

in a future publication. The results presented in the paper should help in the broader adoption of permeation passive sampling in different application areas.

## Acknowledgements

The authors wish to thank Dr. Jacek Namieśnik, Dr. Bożena Zabiegała and Dr. Monika Partyka at the Gdańsk University of Technology for helpful discussions. This work was financially supported by the University Consortium for Field Focused Groundwater Contamination Research and Natural Sciences and Engineering Research Council of Canada (NSERC).

## References

- [1] T. Górecki, J. Namieśnik, Trends Anal. Chem. 21 (2002) 276.
- [2] S. Seethapathy, T. Górecki, X. Li, J. Chromatogr. A 1184 (2008) 234.
- [3] B. Zabiegała, T. Górecki, J. Namieśnik, Anal. Chem. 75 (2003) 3182.
- [4] B. Zabiegała, T. Górecki, E. Przyk, J. Namieśnik, Atmos. Environ. 36 (2002) 2907.
- [5] B. Zabiegała, B. Zygmunt, E. Przyk, J. Namieśnik, Anal. Lett. 33 (2000) 1361.
- [6] B. Zabiegała, J. Namieśnik, E. Przyk, A. Przyjazny, Chemosphere 39 (1999) 2035.
- [7] J.G. Wijmans, J. Membr. Sci. 237 (2004) 39.
- [8] T.C. Merkel, V.I. Bondar, K. Nagai, B.D. Freeman, I. Pinnau, J. Polym. Sci. Part B 38 (2000) 415.
- [9] T. Kotiaho, F.R. Lauritsen, in: D. Barceló (Ed.), Comprehensive Analytical Chemistry, vol. 37, Elsevier, Amsterdam, 2002, p. 535.
- [10] S.V. Dixon-Garret, K. Nagai, B.D. Freeman, J. Polym. Sci. 38 (2000) 1461.
- [11] J.M. Kong, S.J. Hawkes, J. Chromatogr. Sci. 14 (1976) 279.
- [12] J.M. Watson, P.A. Payne, J. Membr. Sci. 49 (1990) 171.
- [13] D.A. Skoog, F.J. Howler, T.A. Nieman, Principles of Instrumental Analysis, 5th ed., Brooks/Cole, Florence, 1998.
- [14] H.V. van Den Dool, P.D. Kratz, J. Chromatogr. 11 (1963) 463.
- [15] F.R. Gonzalez, A.M. Nardillo, J. Chromatogr. A 842 (1999) 29.
- [16] P.A. Martos, A. Saraullo, J. Pawliszyn, Anal. Chem. 69 (1997) 402.
- [17] A. Kłoskowski, W. Chrzanowski, M. Pilarczyk, J. Namieśnik, J. Chem. Therm. 37 (2005) 21.
- [18] C.A. Cramers, C.E. van Tilburg, C.P.M. Schutjes, J.A. Rijks, G.A. Rutten, R. de Jijis, J. Chromatogr. 279 (1983) 3.
- [19] B. Zabiegała, M. Partyka, T. Górecki, J. Namieśnik, J. Chromatogr. A 1117 (2006) 19.
- [20] <http://www.sspinc.com/prodspecs/ssp-m100.cfm> (accessed on 15.07.09).
- [21] J. Namieśnik, Personal Communication, Gdańsk University of Technology, Poland.
- [22] National Institute of Standards and Technology Mass Spectral Database, MS Search 2.0, Gaithersburg, MD.
- [23] D. Monca, L. Feron, J. Weber, Clin. Chem 35/4 (1989) 601.

- [24] [http://massfinder.com/wiki/Retention\\_index\\_guide](http://massfinder.com/wiki/Retention_index_guide) (accessed on 29.08.09).
- [25] E. Boscaini, M.L. Alexander, P. Prazeller, T.D. Maerk, *Int. J. Mass. Spectrom.* 239 (2004) 179.
- [26] C.J. Guo, D. De Kee, *Chem. Eng. Sci.* 46 (1991) 2133.
- [27] E. Favre, P. Schaetzel, Q.T. Nguygen, R. Clement, J. Neel, *J. Membr. Sci.* 92 (1994) 169.
- [28] I. Blume, P.J.F. Schwering, M.H.V. Mulder, C.A. Smolders, *J. Memb. Sci.* 61 (1991) 85.
- [29] C. Dotremont, B. Brabants, K. Geeroms, J. Mewis, C. Vandecasteele, *J. Mem. Sci.* 104 (1995) 109.
- [30] D.A. Skoog, D.M. West, F.J. Holler, S.R. Crouch, *Fundamentals of Analytical Chemistry*, 8th ed., Brooks/Cole, Florence, 2003.
- [31] R.A. Ketola, M. Ojala, H. Sorsa, T. Kotiaho, R.K. Kostianen, *Anal. Chim. Acta* 349 (1997) 359.
- [32] M.J. Yang, S. Harms, Y.Z. Luo, J. Pawliszyn, *Anal. Chem.* 66 (1994) 1339.